Biochemical Engineering Journal 106 (2016) 118–124

Contents lists available at ScienceDirect

Biochemical Engineering Journal

journal homepage: www.elsevier.com/locate/bej

Regular article

Comparison of optimization algorithms for modeling of Haldane-type growth kinetics during phenol and benzene degradation

Su-Youn Kang [a], Sang-Gil Lee [a], Dong-Ju Kim [a,*], Jaemin Shin [b], Junseok Kim [b], Soonjae Lee [c,*], Jae-Woo Choi [c]

[a] Department of Earth and Environmental Sciences, Korea University, Anam Dong 5-1, Seoul 136-701, Republic of Korea
[b] Department of Mathematics, Korea University, Anam Dong 5-1, Seoul 136-701, Republic of Korea
[c] Center for Water Resource Cycle Research, Korea Institute of Science and Technology, Hwarang-ro 14-gil 5, Seongbuk-gu, Seoul 136-791, Republic of Korea

ARTICLE INFO

Article history:
Received 6 May 2015
Received in revised form
29 September 2015
Accepted 19 November 2015
Available online 23 November 2015

Keywords:
Modeling
Optimization
Kinetic parameters
Growth kinetics
Microbial growth
Phenol
Benzene

ABSTRACT

In this study, three optimization algorithms (discretized domain, Monte Carlo, steepest descent) were compared to determine the best algorithm for estimation of Haldane-type microbial growth kinetic parameters. Application of these algorithms to growth data measured during phenol and benzene degradation showed different results in the estimated parameters obtained under various boundary conditions and growth phases. Regardless of the specific algorithm used, the factor with the greatest influence on parameter estimation was the boundary condition for the half-saturation constant (K_S), although the parameters were also sensitive to the growth phase for phenol. Among the three algorithms, Monte Carlo was found to be the best and most consistent. The estimated parameters of phenol and benzene using an appropriate boundary value of K_S were comparable with the outputs reported in previous studies, but those derived with inappropriate boundary values were not consistent with previously reported data.

1. Introduction

Phenol is one of the main toxic organic contaminants frequently detected in industrial effluents. When phenolic wastewater is discharged without treatment, the underground aquifer and ecosystem can be seriously damaged owing to the high solubility and toxicity of phenol. Therefore, numerous studies have been conducted to develop methods for the effective removal of phenol from wastewater, using the adsorption capacity of activated carbon [1], photo-catalysts such as TiO_2 and ZnO [2], and metabolism of phenol by microorganisms [3,4]. Recently, attention in this field has focused on biological treatments, which have advantages with respect to their cost-effectiveness and eco-friendly nature.

The relationship between microbial growth and phenol concentration has been considered to be a key factor in determining the efficiency of treating phenol existing at various concentrations in wastewater. In general, the specific growth rate of a microorganism, μ (1/h), shows a nonlinear relationship with substrate concentration, S (mg/L). Depending on the concentration range used, this nonlinear relationship can be estimated using either noninhibitory or inhibitory kinetic models. The Monod (1) and Haldane (2) models, which are well-known kinetics models used to express the noninhibitory and inhibitory behavior of microorganisms, respectively, can be defined as follows:

$$\mu = \mu_{\max} \frac{S}{K_s + S} \quad (1)$$

$$\mu = \mu_{\max} \frac{S}{K_S + S + S^2/K_I} \quad (2)$$

where $\mu_{\max}$ is the maximum growth rate (1/h), K_S is the half-saturation constant (mg/L), and K_I is the inhibitory constant (mg/L). When the Haldane model is used to estimate kinetic parameters, the change of any one parameter can lead to a simultaneous change of the other two parameters, implying that multiple sets that satisfy the optimization problem can exist for a given experimental dataset.

One way to resolve this dependency problem of estimated parameters would be to use a discretization method by which the parameter domain is discretized so that the effect of the boundary values and intervals on model outputs can be systematically

* Corresponding author.
E-mail addresses: djkim@korea.ac.kr (D.-J. Kim), soonjaemail@gmail.com (S. Lee).

http://dx.doi.org/10.1016/j.bej.2015.11.012
1369-703X/

Table 1
Boundary values and intervals of kinetic parameters used for algorithm optimization.

Constraints			Kinetic parameter					
			μ_{max} (1/h)		K_S (mg/L)		K_I (mg/L)	
Boundary[a]			$a_{1(min)}$	$b_{1(max)}$	$a_{2(min)}$	$b_{2(max)}$	$a_{3(min)}$	$b_{3(max)}$
	Type A	(Phenol)	0	1	0	800	0	800
		(Benzene)	0	1	0	400	0	400
	Type B	(Phenol)	0	1	0	50	0	800
		(Benzene)	0	1	0	15	0	400
Interval[b]	Type A		0.01		10		10	
	Type B		0.01		1		10	
Initial value[c]	(Given)	Optimized parameter set obtained from DD						
	(Random)	Randomly selected values from Eq. (8)						

[a] Boundary values used in DD, MC, SD.
[b] Intervals used in DD.
[c] Initial values used in SD.

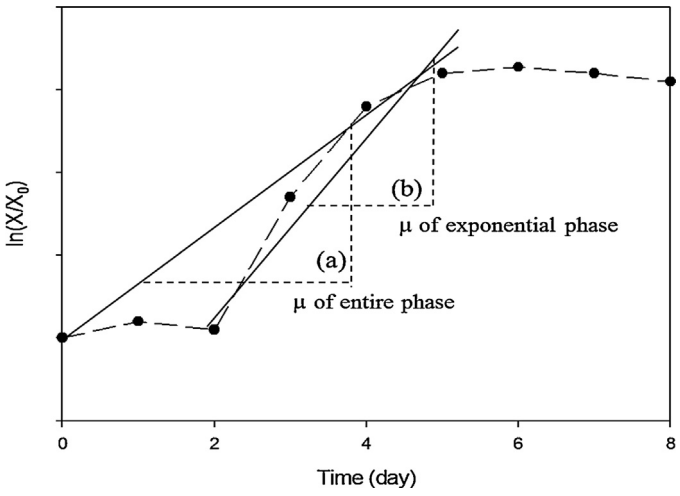

Fig. 1. Effect of growth phase on the determination of specific growth rate (μ).

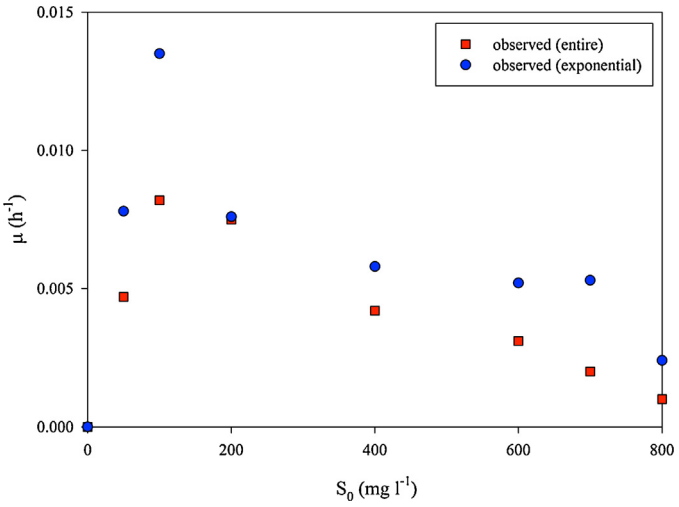

Fig. 2. Comparison of the observed growth rates determined from the entire and exponential growth phases.

explored. For example, the discretized domain (DD) technique was applied to a simulation of a variable and fluctuating traffic signal system [5]. This method was also applied to an unsaturated groundwater flow problem by discretization of variable vertical grid spacing [6]. These exemplary studies indicate that discretization is a useful technique for transferring a continuous parameter domain into discrete points to make it suitable for numerical evaluation. However, the discretization method becomes inefficient when the spacing of grid points is wide or if a solution point exists between grid points. To overcome this problem, the steepest descent (SD) method can be used. SD is a mathematical algorithm in which a sequence series is generated to push the gradient towards the direction that minimizes the value of the error function. Since the determination of the gradient is taken from the mathematical calculation of an earlier step, the entire problem domain has an equal possibility to be tested. The use of the SD technique was reported in a study of the cell growth kinetics during substrate interactions between phenol and *m*-cresol [7].

In addition to these two methods, the Monte Carlo (MC) algorithm is another alternative for simple optimization when a kinetic model is complex, nonlinear, or includes more than two parameters. This method evaluates the error function using a uniform distribution of probability for a given random number by simplifying the mathematical procedure. This simplicity of the MC method was demonstrated in a study of the geophysical inversion problem as a control-searching method to test the effectiveness of complicated algorithms [8].

To date, numerous studies on the estimation of Haldane-type growth kinetic parameters for phenol degradation have been conducted. However, with the exception of only two studies – Alexievaa et al. [17] and Kumar et al. [18] that defined the algorithms of Hooke and Jeeves, and Levenberg-Marquardt, respectively – none of the other studies [19–23] mentioned the specific algorithm used or the associated boundary values of the kinetic parameters. In addition, to our knowledge, no study has been conducted to evaluate the effect of specific optimization algorithms on the estimation of growth kinetic parameters showing a nonlinear inhibitory pattern. Therefore, the aim of this study was to estimate the growth kinetic parameters of two biodegradable organics (phenol and benzene) using three optimization algorithms (DD, SD, and MC) for various boundary values and growth phases.

2. Materials and methods

2.1. Microorganism and culture medium

The bacterial strain *Pseudomonas putida* F1 (Korea National Environmental Microorganisms Bank, Suwon, Korea) was pre-cultured in 2 L of Luria-Bertani medium (10 g/L tryptone, 5 g/L yeast extract, 5 g/L NaCl) at 30 °C in an incubator for 2 days. The bacterial cells in the late exponential growth phase were harvested by centrifugation at 10,000 rpm and 4 °C for 15 min, washed twice with mineral salt medium (MSM), and re-suspended in MSM. The composition of MSM was determined from a previous study [9] as follows (per liter): K_2HPO_4 0.095 g, KH_2PO_4 0.1055 g, $(NH_4)_2SO_4$ 0.488 g, $CaCl_2H_2O$ 3.676 g, $FeCl_36H_2O$ 0.10 g, NaCl 0.060 g, $MgSO_47H_2O$ 0.123 g. The re-suspended cells were adjusted to a final optical den-

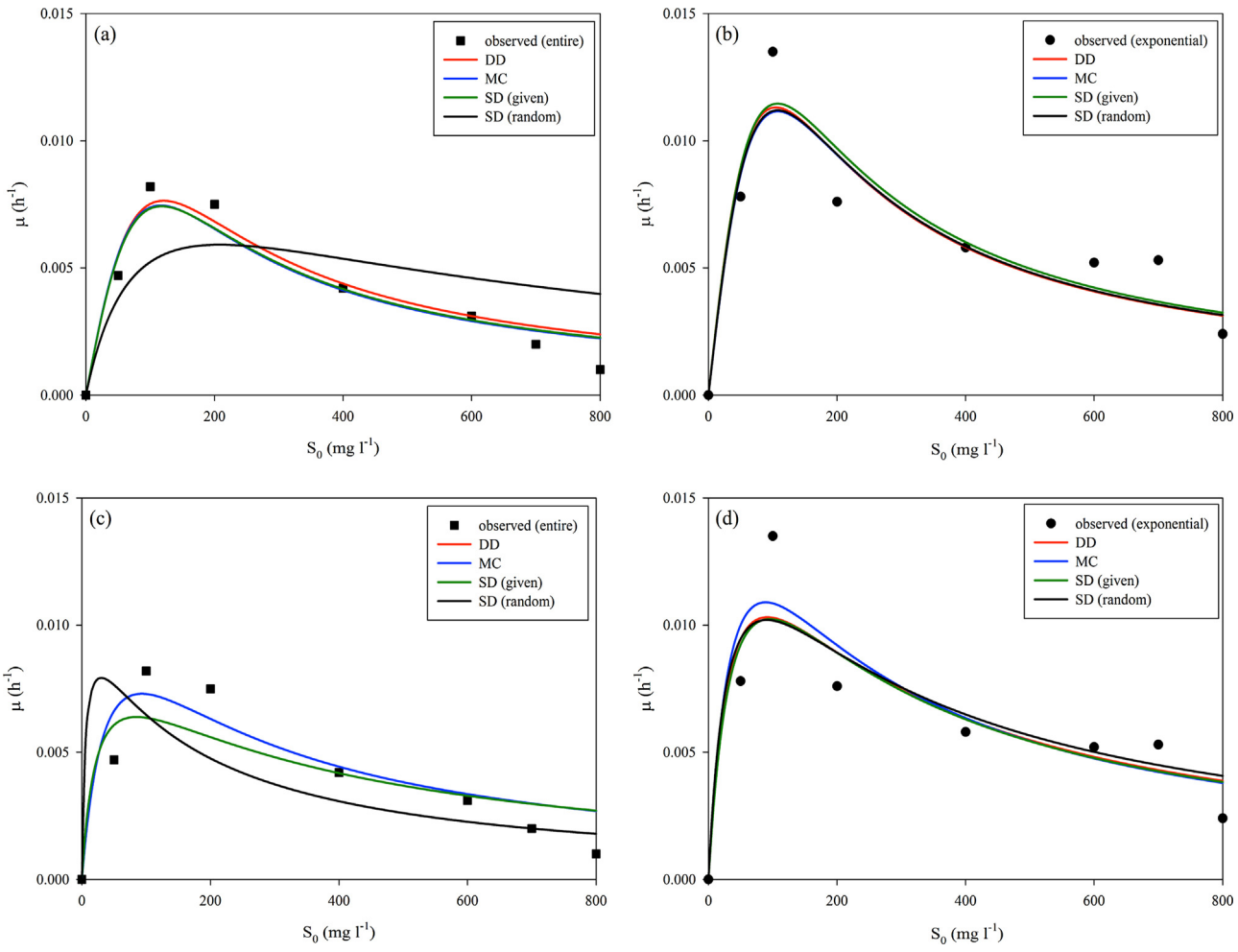

Fig. 3. Fit of the three algorithms to the observed data of phenol with various boundary types and growth phases: (a) boundary type A and entire growth phase, (b) boundary type A and exponential growth phase, (c) boundary type B and entire growth phase, (d) boundary type B and exponential growth phase. DD, discretized domain; MC, Monte Carlo; SD, steepest descent.

sity at 600 nm (OD_{600}) of 0.2, and used as a source of inoculum for the batch experiments.

2.2. Experimental design for the batch test

A batch experiment was conducted to investigate the effect of the initial concentration of phenol on bacterial growth, and to determine the phenol degradation profile for *P. putida* F1. Various concentrations (50, 100, 200, 400, 600, 700, 800 mg/L) of phenol were prepared in 500-mL flasks containing 450 mL of MSM, and the *P. putida* F1 concentration corresponding to an OD_{600} of 0.2 was inoculated into the medium. The culture flasks were sealed with parafilm to prevent contamination in the microcosm. The flasks were shaken at 140 rpm and maintained at 30 °C and pH 7.5 in the shaking incubator until the experiment was complete. The suspension was sampled at pre-determined time intervals (0, 1, 2, 3, 4, 5, 6, 7, 8, 9, 10 days) using a sterilized airtight glass syringe to determine cell growth and phenol concentration. Additional sampling was conducted in the period of abrupt changes in biomass and phenol concentration. A control experiment without the bacterial strain was also conducted to check for any abiotic-derived losses of phenol. All batch experiments were run in quadruplicate.

A batch experiment for benzene was conducted in our previous study [24]. Except for the bacterial strain (*Pseudomonas putida* KCTC-1769) and initial concentration range (30–400 mg/L), the experimental procedure was identical to that described here for phenol.

2.3. Analytical methods

Biomass concentration was determined on a UV-visible spectrophotometer (Helios ß, Thermo-Electron Corporation, MA, USA) at 600 nm by measuring the absorbance of the cell solution. Phenol concentrations were measured using high-performance liquid chromatography (HPLC; Young Lin, Seoul, Korea) equipped with a fluorescence detector (M720), M925 pump, Rheodyne injector, and C18 column (150 × 4.6 mm; Phenomenex, Torrance, CA, USA) at an excitation wavelength of 280 nm. The elution gradient was methanol:distilled water = 4:3 (w/w) with a flow rate of 1.0 mL/min at an oven temperature of 35 °C. A 0.6-mL sample of the working solution was collected using a 1-mL glass syringe, which was then transferred to a 0.5-mL microtube, centrifuged at 3000 rpm for 3 min, and then 8-μL aliquots of the supernatant were injected to the HPLC system.

2.4. Evaluation of the experimental growth curve

The specific growth rate in a batch system is defined as

$$\mu = \frac{1}{X}\frac{dX}{dt} \tag{3}$$

Table 2
Estimated parameters of phenol for two boundary types (A and B) and growth phases (entire and exponential).

Boundary type A	(a) Entire growth phase				(b) Exponential growth phase			
	DD	MC	SD (Given)	SD (Random)	DD	MC	SD (Given)	SD (Random)
μ_{max} (1/h)	0.1	0.11	0.10	0.011	0.13	0.14	0.13	0.14
K_S (mg/L)	730	799	734	89.6	550	623	556	618
K_I (mg/L)	20	16.9	18.9	483	20	18.7	20.8	18.7
$e(p)$	4.0E-06	4.0E-06	4.0E-06	2.9E-05	1.4E-05	1.4E-05	1.4E-05	1.4E-05
Boundary type B	(a) Entire growth phase				(b) Exponential growth phase			
	DD	MC	SD (Given)	SD (Random)	DD	MC	SD (Given)	SD (Random)
μ_{max} (1/h)	0.01	0.015	0.010	0.011	0.02	0.023	0.021	0.018
K_S (mg/L)	24	49.1	24.0	5.85	43	49.3	50	34.6
K_I (mg/L)	300	177	300	156	195	160	181	237
$e(p)$	1.3E-05	9.6E-06	1.3E-05	2.2E-05	1.8E-05	1.8E-05	1.8E-05	1.9E-05

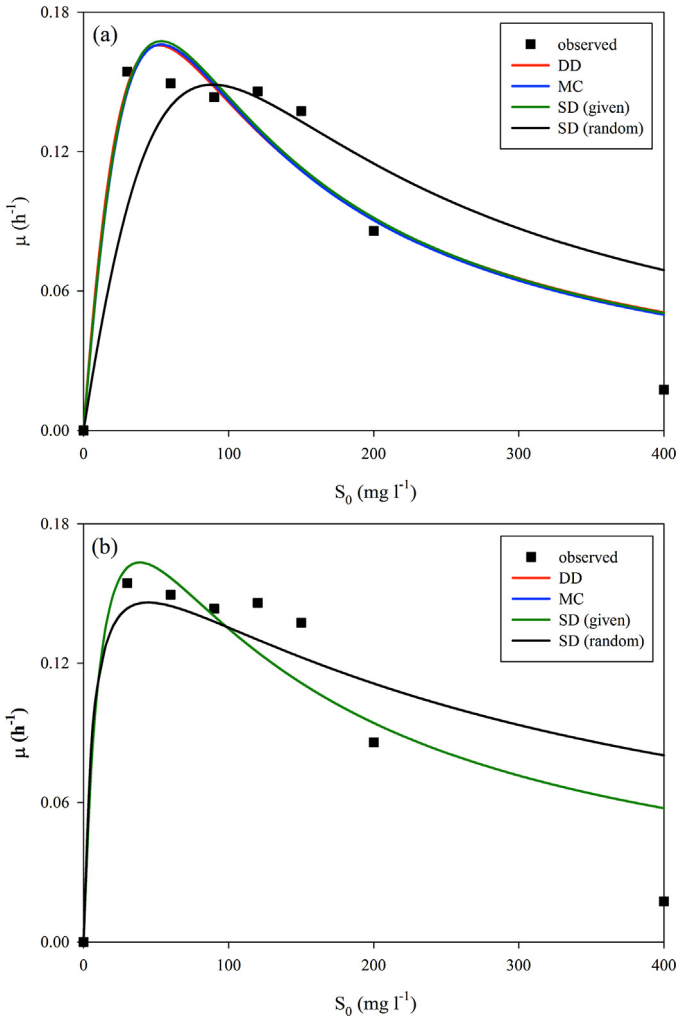

Fig. 4. Fit of the three algorithms to the observed data of benzene with various boundary types: (a) boundary type A, (b) boundary type B. DD, discretized domain; MC, Monte Carlo; SD, steepest descent.

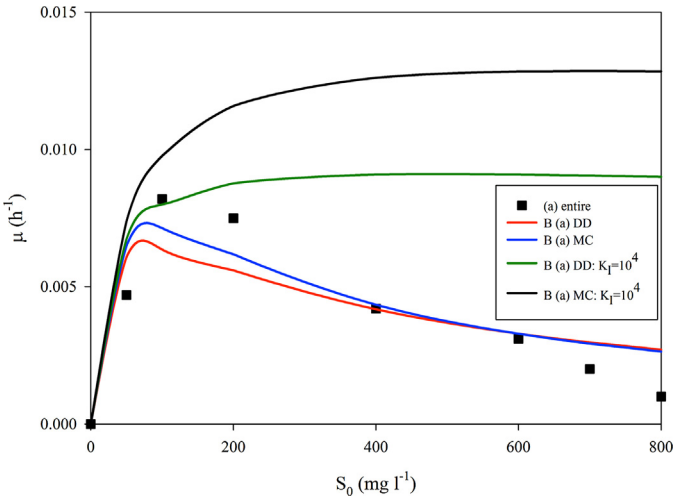

Fig. 5. Simulation of growth curves using Monod kinetics to estimate an appropriate K_S value. DD, discretized domain; MC, Monte Carlo; SD, steepest descent.

where X is the OD_{600} of biomass. After the values of μ were determined from the slope of the logarithm of the plot of X/X_0 versus time for each initial concentration of phenol (S), a Haldane kinetic model was fit to the μ–S relationship. In this study, we defined two different growth stages, (a) entire and (b) exponential phase, for parameter estimation, since the determination of μ was affected by the stage of growth (Fig. 1).

2.5. Optimization algorithms

The Haldane function is denoted as $\mu = f(s; p)$, where the vector p represents the parameters such as $p = (\mu_{max}, K_S, K_I)$. The parameter domain is constrained so that $\Omega = [a_1, b_1] \times [a_2, b_2] \times [a_3, b_3]$ for μ_{max}, K_S, and K_I in three-dimensional space, where the values of a_n and b_n are the minimum and maximum boundaries, respectively. For m experimental data, $E = \{(S_i, \mu_i) | i = 1, \ldots, m\}$ is denoted as the set of the data. Then, the error function is defined as

$$e(p) = \sum_{i=1}^{m} |\mu_i - f(s_i; p)|^2 \quad (4)$$

Three optimization algorithms were used to determine the best parameters that could minimize $e(p)$ for given parameter domain Ω.

The two different types of boundaries and intervals used for the optimization algorithms are listed in Table 1. Of note, 800 mg/L and 10 mg/L were used as the maximum boundary and interval of K_S for type A, whereas 50 mg/L and 1 mg/L were used for the minimum boundary and interval for type B. For the case of benzene, the maximum boundary of K_S was used 400 and 15 mg/L for type A and B, respectively. For the initial state of the SD model, two strategies

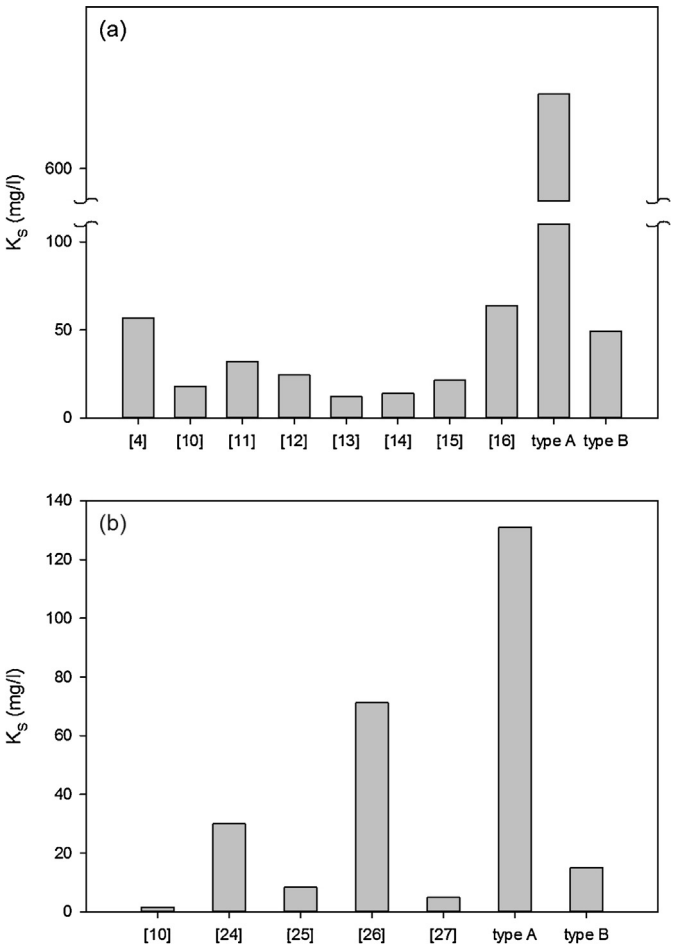

Fig. 6. Comparison of K_S values obtained in this study and in previous studies: (a) phenol degradation, (b) benzene degradation.

were adopted: p° that minimizes $e(p)$ at the target points of Ω_d (given), and p° that is randomly selected by Ω_r (random).

2.5.1. Discretized domain (DD)

For discretization of the parameter domain, let N_1, N_2, and N_3 be positive integers and

$$\Omega_d = \{(x_i, y_j, z_k) \,|x_i = a_1 + \frac{i}{N_1}(b_1 - a_1), y_j = a_2 + \frac{j}{N_2}(b_2 - a_2),$$

$$z_k = a_3 + \frac{k}{N_s}(b_3 - a_3), 0 \le i \le N_1, 0 \le j \le N_2, 0 \le k \le N_3\} \quad (5)$$

be the set of mesh grid points. Then, the minimum error was approximated by $\min_{p \in \Omega_r} e(p)$and values corresponding to this error were chosen to be the best parameter set.

2.5.2. Monte Carlo (MC)

Monte Carlo was considered as

$$\Omega_r = \{(x_i, y_i, z_i) \,|x_i = a_1 + (b_1 - a_1)rand(x_i),$$

$$y_i = a_2 + (b_2 - a_2)rand(y_i), z_i = a_3 + (b_3 - a_3)rand(z_i)\}, \quad (6)$$

where rand $(\cdot)$ is a uniformly distributed random number between 0 and 1. Then, the optimal parameter set that satisfies $\min_{p \in \Omega_r} e(p)$as found.

2.5.3. Steepest descent (SD)

To minimize $e(p)$, the SD method generated a sequence $\{p^k\}$ such that

$$p^{k+1} = p^k - \alpha_k \nabla e(p^k). \quad (7)$$

For $k = 0, 1, \cdots$, where α_ks the value that minimizes the function $h(\alpha)$defined by

$$h(\alpha) = e\left(p^k - \alpha \nabla e\left(p^k\right)\right), \quad (8)$$

the gradient is approximated as

$$\nabla e\left(p^k\right) = \left(\frac{e\left(p^k + \varepsilon u_1\right) - e\left(p^k - \varepsilon u_1\right)}{2\varepsilon}, \right.$$

$$\left. \frac{e\left(p^k + \varepsilon u_2\right) - e\left(p^k - \varepsilon u_2\right)}{2\varepsilon}, \frac{e\left(p^k + \varepsilon u_3\right) - e\left(p^k - \varepsilon u_3\right)}{2\varepsilon} \right), \quad (9)$$

where ε is a sufficiently small value, andu_1, u_2, and u_3 are the unit vectors for x, y, and z, respectively. The quadratic polynomial $q(\alpha)$ as constructed, which interpolates h at α_k^1, α_k^2, and$\alpha_k^3(\alpha_k^1 < \alpha_k^2 < \alpha_k^3)$. Then, α_k was defined by the minima of $q(\alpha)$ to approximate the minimal value of $h(\alpha)$

3. Results and discussion

3.1. Microbial growth kinetics for the phenol degradation

3.1.1. Determination of the specific growth rate

The specific growth rate μ was determined from two different growth stages, entire and exponential phase. The observed growth rates from the different growth phase are compared in Fig. 2. The growth rate from the exponential phase showed more scattering with a higher peak than that obtained from the entire growth phase. The lower value of the growth rate estimated from the entire phase is because the lag period is also included in the time for microbial growth as shown in Fig. 1.

3.1.2. Comparison of the growth kinetics optimized using different algorithms

The growth kinetics for phenol degradation determined using the different four optimization algorithms are demonstrated in Fig. 3 by comparison in two different growth phases (entire vs. exponential) and two boundary types (A and B). The model fitting of the data from the entire growth phase (Fig. 3a and c) was sensitive to the algorithm used; in an extreme case, the model fit by SD (random) completely failed to depict the growth data. Although the application of the type B boundary to the entire growth phase data could improve the goodness of fit of SD (random), the fitted growth kinetics was significantly different from with the others as before. In contrast, the model fitting of the growth rate data from the exponential growth phase (Fig. 3b and d) showed that all three optimization algorithms, including SD (random), could fit the data equally well, regardless of boundary type.

Overall, the performance of the optimization algorithm was dependent on growth phase as well as boundary type. The effect of boundary type was more pronounced for the entire growth phase data, in which switching to boundary type B showed better performance of the model fit by the SD (random) algorithm. Nevertheless, the three optimization algorithms showed equally good performance regardless of boundary type for the data of the exponential growth phase, although there was a slight difference between the peaks of the Haldane-type models. This indicates that the specific growth rate determined from the exponential growth phase could derive more stable and consistent results.

Table 3
Estimated parameters of benzene for two boundary types (A and B) at the exponential growth phase.

	Boundary type A				Boundary type B			
	DD	MC	SD (Given)	SD (Random)	DD	MC	SD (Given)	SD (Random)
μ_{max} (1/h)	0.74	0.98	0.96	1.00	0.29	0.29	0.29	0.19
K_S (mg/L)	90.0	130.8	126.4	254.0	15.0	15.0	15.0	6.67
K_I (mg/L)	30.0	21.8	22.6	31.1	100.0	100.0	100.0	296.8
$e(p)$	2.4E-03	2.4E-03	2.4E-03	7.12E-03	2.9E-03	2.9E-03	2.9E-03	5.2E-03

Table 4
Comparison of Haldane growth kinetic parameters of phenol obtained in this study and in previous studies.

Strain		Kinetic parameters			Concentration range	Reference
		μ_{max} (1/h)	K_S (mg/L)	K_I (mg/L)	(mg/L)	
Pseudomonas sp.		0.27	56.7	249	100–500	[4]
P. putida F1		0.051	18	430	10–200	[10]
P. putida F1		0.11	32	–	54	[11]
P. putida LY1		0.22	24.4	122	0–800	[12]
P. putida CCRC		0.24	12.1	1184	0–400	[13]
P. putida CCRC		0.33	13.9	669	25–600	[14]
P. putida		0.47	21.5	478	50–250	[15]
P. putida PTCC		0.031	63.9	450	300–1000	[16]
[a]*P. putida*	Type A	0.014	623	18.7	50–800	This study
F1	Type B	0.028	49.3	160		

[a] determined using the growth rates data from the exponential growth phase.

Table 5
Comparison of Haldane growth kinetic parameters of benzene obtained in this study and in previous studies.

Strain	Kinetic parameters			Concentration range	Reference
	μ_{max} (1/h)	K_S (mg/L)	K_I (mg/L)	(mg/L)	
P. putida F1	0.62	1.65	180	3–187.7	[10]
P. putida KCTC-40269	0.3	30	100	30–400	[24]
P. sp. NCIMB-9688	0.0094	8.30	158	200	[25]
P. putida MTCC-1194	0.1631	71.18	340.15	50–300	[26]
P. sp. YATO411	0.1155	4.93	52.63	17.6–52.7	[27]
P. putida F1	0.29	15	100	30–400	This study

The estimated parameters of phenol are listed in Table 2. Different parameter sets were obtained depending on the optimization algorithm, growth phase, and boundary type applied. For boundary type A and data from the entire growth phase, a substantial difference was observed in the SD (random), where μ_{max} and K_S decreased by 10- and 8-fold, respectively, whereas K_I increased by 24-fold compared to these values obtained with DD, MC, and SD (given). For boundary type A and the exponential growth phase data, the values of μ_{max}, K_S, and K_I were in the range of 0.13–0.14 1/h, 550–623 mg/L, and 18.7–20.8 mg/L, respectively, with an identical $e(p)$ value. For boundary type A, switching from the entire to exponential growth phase resulted in an increase of μ_{max} by 1.3-fold (from 0.10–0.11 to 0.13–0.14 1/h) but a decrease of K_S by 1.3-fold (from 730 to 799 to 550–623 mg/L) due to the increase in the peak of the specific growth rate. By contrast, the values of K_I were nearly constant, at 16.9–20.8 mg/L. For the exponential phase, switching from boundary type A to B resulted in a decrease in both μ_{max} and K_S by 6.5- and 12.7-fold, respectively, but led to an increase of K_I by 8.5-fold. Therefore, boundary type caused more substantial variation in K_S than did growth phase.

For both growth phases, the estimated parameters for boundary type B showed a decrease of μ_{max} and K_S, and an increase of K_I compared to boundary type A. This may be due to the interdependency between Haldane parameters to compensate for the change of K_S, which is restricted to the lower range in boundary type B ($0 \le K_S \le 50$). Considering the range of estimated parameters, the optimization results obtained when using boundary type B seem to be more reliable. For instance, the range of parameter values for K_I of boundary type A (16.9–20.8 mg/L), with the exception of SD (random), was unrealistic compared to that obtained with type B (K_I = 160–300 mg/L), since the observed data showed inhibitory behavior at concentrations of 100–200 mg/L.

The parameters and fitting curves from SD (random) method were significantly different to those from DD and MC methods. In contrast, DD and MC methods obtained similar parameters and fitting curves in Table 2 and Fig. 3(a–d), respectively. Indeed, SD method finds a local minimum, which depends on the initial values, even though this method is efficient. The reason of similarity in the obtained parameters from DD and MC methods is that these two methods find global minimum approximately, and each minimum is independent on the initial values for the parameters. To enhance the precision of the minima, we can use DD method with finer-grid domain or MC method with a greater number of trials.

SD (given) is another approach to enhance the precision of the set of parameters. As we mentioned, the parameter set obtained from DD was adopted to the initial estimates for SD (given). Since this approach finds local minimum around the initial value which is the approximated global minimum from DD method, the set of parameters from SD (given) is better than those from SD (random) and DD methods.

3.2. Microbial growth kinetics for the benzene degradation

The comparison between optimization algorithms for benzene is also shown in Fig. 4. Model fitting to the exponential growth data showed that all three models, except for SD (random), could fit to

the data equally well, regardless of boundary type. The estimated parameters of benzene are listed in Table 3. For boundary type A, the values of K_S were in the range of 90–254 mg/L, and switching from boundary type A to type B resulted in a 68.7-fold decrease in K_S to 6.6–15 mg/L. This decrease of K_S invoked a decrease of μ_{max} and an increase of K_I, as observed in the case of phenol. It is remarkable that all three algorithms gave an identical result. This is because the minimum $e(p)$ happens to appear exactly on the grid of the discretized parameter domain.

3.3. Appropriateness of the estimated K_S

In order to determine the appropriate value of K_S for phenol, a noninhibitory growth curve was generated using Monod kinetics (Fig. 5). For the simulation of growth rate by Monod kinetics, the values of K_I for DD and MC increased to be sufficiently high ($K_I = 10^4$ mg/L $\approx \infty$). This revealed that K_S, the substrate concentration corresponding to half the value of μ_{max}, could be estimated at 50 mg/L for both DD and MC. Taking this value into account, the K_S value (24 mg/L) obtained with the DD algorithm appears to have been underestimated, whereas that obtained with the MC algorithm was adequately estimated (49.1 mg/L). The estimated parameters of the exponential growth phase using the MC algorithm were $\mu_{max} = 0.14$ 1/h, $K_S = 623$ mg/L, $K_I = 18.7$ mg/L for boundary type A, and $\mu_{max} = 0.023$ 1/h, $K_S = 49.3$ mg/L, $K_I = 159$ mg/L for boundary type B. The overestimation of K_S when employing boundary type A is depicted in Fig. 6 for phenol and benzene, based on comparison with values reported in the literature (Tables 4 and 5). For both phenol and benzene, selection of type A (imposition of the K_S upper boundary to the maximum test concentration [800 mg/L phenol, 400 mg/L benzene]) resulted in exceptionally high values of K_S with low K_I values, all of which fell out of the reasonable range. Therefore, appropriate imposition of the boundary value of K_S was determined to be the most essential factor in the modeling of Haldane-type growth kinetics for the two model compounds tested here, phenol and benzene.

4. Conclusions

Different optimization algorithms, DD, MC, and SD, were compared in terms of boundary values and growth phase (entire vs. exponential phase) in order to select the best optimization algorithm for the determination of Haldane-type growth kinetic parameters of phenol and benzene, which showed inhibitory kinetics at high concentration ranges. The results revealed that the maximum boundary value of K_S (i.e., the half-saturation constant) was the most important factor influencing suitable growth parameter estimation, since reducing the boundary to a reasonable value resulted in more reliable K_S values. Application of these three algorithms (DD, MC, SD) to benzene and phenol dynamics showed that the same output was obtained with all three algorithms for benzene, whereas the MC algorithm provided more consistent kinetic parameters for the phenol data obtained from both the entire and exponential microorganism growth phases.

Acknowledgement

The authors appreciate the special fund (K1400687) granted by Korea University.

References

[1] N. Tancredi, N. Medero, F. Möller, J. Píriz, C. Plada, T. Cordero, Phenol adsorption onto powdered and granular activated carbon prepared from *Eucalyptus* wood, J. Colloid Interface Sci. 279 (2004) 357–363.
[2] Q. Zhang, W. Fan, L. Gao, Anatase TiO_2 nanoparticles immobilized on ZnO tetrapods as a highly efficient and easily recyclable photocatalyst, Appl. Catal. B: Environ. 76 (2007) 168–173.
[3] A. Banerjee, A.K. Ghoshal, Isolation and characterization of hyper phenol tolerant *Bacillus* sp. from oil refinery and exploration sites, J. Hazard. Mater. 176 (2010) 85–91.
[4] P. Polymenakou, E. Stephanou, Effect of temperature and additional carbon sources on phenol degradation by an indigenous soil *Pseudomonad*, Biodegradation 16 (2005) 403–413.
[5] J.Q. Li, Discretization modeling, integer programming formulations and dynamic programming algorithms for robust traffic signal timing, Transp. Res. Part C: Emerg. Technol. 19 (2011) 708–719.
[6] J.J. Carrera-Hernández, B.D. Smerdon, C.A. Mendoza, Estimating groundwater recharge through unsaturated flow modelling: sensitivity to boundary conditions and vertical discretization, J. Hydrol. 452–453 (2012) 90–101.
[7] J. Bai, J.P. Wen, H.M. Li, Y. Jiang, Kinetic modeling of growth and biodegradation of phenol and m-cresol using *Alcaligenes faecalis*, Process Biochem. 42 (2007) 510–517.
[8] S. Horne, C. MacBeth, A comparison of global optimization methods for near-offset VSP inversion, Comput. Geosci. 24 (1998) 563–572.
[9] A. Mordocco, C. Kuek, R. Jenkins, Continuous degradation of phenol at low concentration using immobilized *Pseudomonas putida*, Enzyme Microb. Technol. 25 (1999) 530–536.
[10] T. Abuhamed, E. Bayraktar, T. Mehmetoglu, U. Mehmetoglu, Kinetics model for growth of *Pseudomonas putida* F1 during benzene, toluene and phenol biodegradation, Process Biochem. 39 (2004) 983–988.
[11] K.F. Reardon, D.C. Monsteller, J.D. Bull Rogers, Biodegradation kinetics of benzene, toluene, and phenol as single and mixed substrate for *Pseudomonas putida*, Biotechnol. Bioeng. 69 (2000) 385–400.
[12] Y. Li, J. Li, C. Wang, P. Wang, Growth kinetics and phenol biodegradation of psychrotrophic *Pseudomonas putida* LY1, Bioresour. Technol. 101 (2010) 6740–6744.
[13] R.S. Juang, S.Y. Tsai, Enhanced biodegradation of mixed phenol and sodium salicylate by *Pseudomonas putida* in membrane contactors, Water Res. 40 (2006) 3517–3526.
[14] H.Y. Chung, Mass transfer effect and intermediate detection for phenol degradation in immobilized *Pseudomonas putida* systems, Process Biochem. 38 (2003) 1497–1507.
[15] V. Vijayagopal, T. Viruthagiri, Batch kinetic studies in phenol biodegradation and comparison, Ind. J. Biotechnol. 4 (2005) 565–567.
[16] Z. Bakhshi, G. Najafpour, E. Kariminezhad, R. Pishgar, N. Mousavi, T. Taghizade, Growth kinetic models for phenol biodegradation in a batch culture of *Pseudomonas putida*, Environ. Technol. 32 (2011) 1835–1841.
[17] Z. Alexievaa, M. Gerginova, P. Zlateva, N. Peneva, Comparison of growth kinetics and phenol metabolizing enzymes of *Trichosoporoncutaneum* R57 and mutants with modified degradation abilities, Enzyme Microbial Technol. 34 (2004) 242–247.
[18] A. Kumar, S. Kumar, S. Kumar, Biodegradation kinetics of phenol and catechol using *Pseudomonas putida* MTCC 1194, Biochem. Eng. J. 22 (2005) 151–159.
[19] J. Yan, W. Jianping, L. Hongmei, Y. Suliang, H. Zongding, The biodegradation of phenol at high initial concentration by the yeast *Candida tropicalis*, Biochem. Eng. J. 24 (2005) 243–247.
[20] P. Saravanan, K. Pakshirajajan, P. Saha, Growth kinetics of an indigenous mixed microbial consortium during phenol degradation in a batch reactor, Bioresour. Technol. 99 (2008) 205–209.
[21] M. Bajaj, C. Gellert, J. Winter, Phenol biodegradation kinetics of an aerobic mixed culture, Biochem. Eng. J. 46 (2009) 205–209.
[22] A. Banerjee, A.K. Ghoshal, Phenol degradation by *Bacillus cereus*: pathway and kinetic modeling, Bioresour. Technol. 101 (2010) 5501–5507.
[23] A. Banerjee, A.K. Ghoshal, Phenol degradation performance by isolated *Bacillus cereus* immobilized in alginate, Int. Biodegrad. Biodeterior. 65 (2011) 1052–1060.
[24] D.J. Kim, J. Choi, N. Choi, B. Mahendran, C. Lee, Modeling of growth kinetics for *Pseudomonas* spp during benzene degradation, Appl. Microbial. Biotechnol. 69 (2005) 456–462.
[25] A. Monero, L. Lanza, M. Zilli, L. Sene, A. Converti, Batch kinetics of *Pseudomonas* sp growth on benzene: modeling of product and substrate inhibitions, Biotechnol. Prog 19 (2003) 676–679.
[26] A.K. Mathur, C.B. Majumder, Kinetics modelling of the biodegradation of benzenetoluene and phenol as single substrate and mixed substrate by using *Pseudomonas putida*, Chem. Biochem. Eng. Q. 24 (2010) 101–109.
[27] S.L. Tsai, C.W. Lin, C.H. Wu, C.M. Shen, Kinetics of xenobiotic biodegradation by the *Pseudomonas* sp YATO411 strain in suspension and cell-immobilized beads, J. Inst. Chem. Eng. 44 (2013) 303–309.